Paramagnetic Resonance and Relaxation of Trivalent Rare-Earth Ions in Calcium Fluoride. II. Spin-Lattice Relaxation

R. W. Bierig, M. J. Weber, and S. I. Warshaw
Raytheon Research Division, Waltham, Massachusetts
(Received 3 January 1964)

The temperature dependence of the spin-lattice relaxation time T_1 of trivalent rare-earth impurities in CaF_2 has been measured at 9.6 kMc/sec using pulse saturation techniques. The rare earths investigated include Kramers ions (Ce^{3+}, Nd^{3+}, Dy^{3+}, Er^{3+}, Yb^{3+}), one non-Kramers ion (Tb^{3+}), and one S-state ion (Gd^{3+}). The relaxation of ions in lattice sites of cubic, tetragonal, and trigonal crystal-field symmetries have been studied and are found to be different. At liquid-helium temperatures the relaxation usually exhibits a T^{-1} temperature dependence; however, the magnitudes are approximately two orders-of-magnitude shorter than estimated single-phonon relaxation times based upon the orbit-lattice interaction. Measurements of the Ce^{3+} relaxation in five samples containing from 0.08 to 1.6% Ce combined with results from other ions show that T_1 decreases with increasing rare-earth concentration. Multiple exponential recoveries from saturation are observed at low temperatures and are discussed with respect to possible cross-relaxation within inhomogeneous spin systems and to other faster relaxing systems. At higher temperatures examples of both Raman and Orbach two-phonon relaxation processes are found. Calculations of two-phonon relaxation times using estimated values of the dynamic crystal fields, energy level structures, and ion wave functions yield coarse order-of-magnitude agreement with experimental values.

INTRODUCTION

SPIN-LATTICE relaxation of rare-earth ions has been the subject of considerable attention in the past few years, prompted by the discovery of the importance of two-step relaxation processes involving low-lying excited states[1] and the subsequent theoretical treatment by Orbach.[2] The relaxation of several different rare-earth ions has been measured in ethyl sulfate,[3] double nitrate,[3] and garnet crystals[4] and compared with theory with varying degrees of success. We have investigated the temperature dependence of the spin-lattice relaxation time, T_1, of trivalent rare-earth ions in CaF_2, including examples of Kramers (Ce^{3+}, Nd^{3+}, Dy^{3+}, Er^{3+}, Yb^{3+}), non-Kramers (Tb^{3+}) and S-state (Gd^{3+}) ions. This crystal is of additional interest since trivalent rare earths can enter the lattice substitutionally in sites having cubic, tetragonal, and trigonal crystal-field symmetry; thus one can compare the characteristics of the relaxation of ions in different symmetry sites in the same host lattice.

Calculations of the rate of spin-lattice relaxation and predictions of the relative importance of various relaxation mechanisms require knowledge of the energy level structures, ion wave functions, and strength of dynamic crystalline fields. Unfortunately, such information is not well established for most rare-earth ions in CaF_2. In the preceding paper[5] (henceforth referred to as I), available optical and electron paramagnetic resonance data were reviewed to obtain estimates of the cubic- and axial-crystal-field parameters and electronic energy levels. These results are used to estimate the magnitude and importance of various one- and two-phonon relaxation processes. Pertinent details of the resonance spectra, g values, etc., are also given in I.

The temperature dependence of T_1 for the above rare-earth ions has been measured from 2°K to as high a temperature as the time resolution (~ 3 μsec) and signal amplitude would permit. These results are presented following a brief review of the theory of spin-lattice relaxation in CaF_2 arising from modulation of the crystal field by thermal lattice vibrations and a discussion of the experimental approach. The T_1's at liquid-helium temperatures usually exhibit a T^{-1} temperature dependence characteristic of one-phonon relaxation processes; however, the magnitudes are about two orders-of-magnitude shorter than estimated relaxation times based upon the orbit-lattice interaction. In the case of Ce^{3+}, the low-temperature relaxation times are found to be a function of rare-earth concentration. Some possible mechanisms which may account for the enhanced and concentration-dependent relaxation rates are discussed qualitatively. At higher temperatures T_1 decreases rapidly with increasing temperature. In most cases the magnitude and temperature dependence of the relaxation times are in reasonable order-of-magnitude agreement with those for two-phonon Orbach and Raman processes calculated by using estimates of the crystal-field parameters and energy level splittings obtained in I.

THEORY

We are interested in the spin-lattice relaxation rate of the lowest resonant doublet of a rare-earth ion in a crystal field. Since no evidence of a phonon bottleneck[3] was observed in our experiments, we shall be concerned with the true spin-lattice rather than the lattice-bath relaxation rate. If the excited states are relatively far removed from the resonant ground doublet, then, following a short intense rf pulse applied to excite the spin

[1] C. B. P. Finn, R. Orbach, and W. P. Wolf, Proc. Phys. Soc. (London) **77**, 261 (1961).
[2] R. Orbach, Proc. Roy. Soc. (London) **A264**, 458 (1961).
[3] P. L. Scott and C. D. Jeffries, Phys. Rev. **127**, 32 (1962) and references therein.
[4] I. Svare and G. Seidel, *Paramagnetic Resonance* (Academic Press Inc., New York, 1963), p. 430.
[5] M. J. Weber and R. W. Bierig, Phys. Rev. **134**, A1492 (1964).

system from its equilibrium Boltzmann population, this two-level system will exhibit a simple exponential recovery with a characteristic time T_1.

There are several spin-lattice relaxation mechanisms which may be operative for rare-earth ions. The theory of rare-earth-ion relaxation has been developed by Orbach[2] and reviewed by Scott and Jeffries.[3] We shall only quote the final results here; the reader is referred to the above papers for more detail.

The simplest relaxation mechanism is a one-phonon direct process in which the spin-relaxation transition is accompanied by the absorption or emission of a single, energy-conserving phonon. The expression for T_1 due to the interaction between a spin and the fluctuating electric crystal field is given by

$$\frac{1}{T_{1D}}=\frac{3}{2\pi\rho v^5\hbar}\left(\frac{\delta}{\hbar}\right)^3|\langle a|\sum_{n,m}V_n{}^m|b\rangle|^2\coth(\delta/2kT), \quad (1)$$

where ρ is the mass density of the sample, v an average phonon velocity, δ the energy of the resonant transition between spin states $|a\rangle$ and $|b\rangle$, and the $V_n{}^m$'s are components of the dynamic crystal-field potential. The orbit-lattice interaction does not connect time conjugate states; consequently, if $|a\rangle$ and $|b\rangle$ are zero-order state functions, Eq. (1) is applicable only to non-Kramers ions, since for a Kramers ion the ground state is at least doubly degenerate and the crystal-field interaction between these states obviously vanishes. A Zeeman field may, however, admix states of the ground doublet with an excited state $|c\rangle$ at an energy Δ_c. Spin-lattice relaxation transitions are now allowed at a reduced rate governed by the magnitude of the Zeeman perturbation and given by

$$\frac{1}{T_{1D}}=\frac{3}{2\pi\rho v^5\hbar}\left(\frac{\delta}{\hbar}\right)^3\left(\frac{2\beta\Lambda}{\Delta^c}\right)^2\{|\langle a|\mathbf{H}\cdot\mathbf{J}|c\rangle\langle c|\sum_{n,m}V_n{}^m|b\rangle$$
$$+\langle a|\sum_{n,m}V_n{}^m|c\rangle\langle c|\mathbf{H}\cdot\mathbf{J}|b\rangle|\}^2\coth(\delta/2kT), \quad (2)$$

where one must sum over all effective states $|c\rangle$. At temperatures above $\sim 1°$K, δ is usually $\ll 2kT$ and hence the direct process relaxation time, T_{1D}, is characterized by a T^{-1} temperature dependence.

An important relaxation mechanism for many rare-earth ions is the so-called Orbach process. This is essentially a two-step process involving real transitions to and from an excited state $|c\rangle$ accompanied by the creation and annihilation of two high-energy phonons. For this mode of resonance relaxation between the phonons and crystal-field splitting, one requires $\Delta_c<k\theta$ where θ is related to the cutoff frequency for phonons and is approximated by the Debye θ. The relaxation rate for this process is

$$\frac{1}{T_{1O}}=\frac{3}{2\pi\rho v^5\hbar}\left(\frac{\Delta_c}{\hbar}\right)^3$$
$$\times\frac{|\sum_{\substack{n,n'\\m,m'}}\langle a|V_n{}^m|c\rangle\langle c|V_{n'}{}^{m'}|b\rangle|^2}{|\sum_{n,m}\langle a|V_n{}^m|c\rangle|^2+|\sum_{n',m'}\langle c|V_{n'}{}^{m'}|b\rangle|^2}$$
$$\times\left(\exp\frac{\Delta_c}{kT}-1\right)^{-1} \quad (3)$$

and is characterized by an exponential temperature dependence at low temperatures, $T\ll(\Delta_c/k)$.

A two-phonon Raman relaxation process is one in which the energy of the spin transition is conserved during an inelastic phonon scattering. If the first-order term in the dynamic crystal-field interaction is used in second-order perturbation theory to calculate the transition probability, one finds that for non-Kramers ions at low temperatures, where $T\ll\theta$,

$$\frac{1}{T_{1R}}=\frac{9\times 6!}{4\rho^2\pi^3v^{10}\Delta_c{}^2}|\sum_{\substack{n,m\\n',m'}}\langle a|V_n{}^m|c\rangle\langle c|V_{n'}{}^{m'}|b\rangle|^2$$
$$\times\left(\frac{kT}{\hbar}\right)^7. \quad (4)$$

For Kramers ions, again due to the consequences of time-reversal symmetry, there is a partial "Van Vleck cancellation"[6] such that in place of Eq. (4) one has

$$\frac{1}{T_{1R}}=\frac{9!\hbar^2}{\pi^3\rho^2v^{10}\Delta_c{}^2}|\sum_{\substack{n,m\\n',m'}}\langle a|V_n{}^m|c\rangle\langle c|V_{n'}{}^{m'}|b\rangle|^2\left(\frac{kT}{\hbar}\right)^9. \quad (5)$$

Another two-phonon Raman contribution arises from the use of the second-order term, in the variation of the crystal field caused by lattice vibrations, in first-order perturbation theory and is given by

$$\frac{1}{T_{1R}}=\frac{9\times 6!}{4\rho^2\pi^3v^{10}}|\sum_{n,m}\langle a|V_n{}^m|b\rangle|^2\left(\frac{kT}{\hbar}\right)^7, \quad (6)$$

for non-Kramers ions at low temperatures. This term is the same order of magnitude and additive to the result in Eq. (4). As for the direct process, the above interaction is active for Kramers ions only via the eigenstate admixing caused by the Zeeman field. This introduces a multiplicative factor, $(2\Lambda\beta H/\Delta_c)^2$, into Eq. (6). In general, the dominant Raman relaxation process for Kramers ions is given by Eq. (5) with a T_{1R} proportional to T^{-9} compared to the T^{-7} temperature dependence for non-Kramers ions.

When a four-level Γ_8 quartet is lowest or in the case of an S-state ion, the effective spin system may not

[6] J. H. Van Vleck, Phys. Rev. **57**, 426 (1940).

consist simply of a single isolated doublet. The relaxation modes in such multilevel systems are, in general, more complex. At low temperatures the dominant relaxation process between pairs of levels may occur via multistep direct processes and exhibit a transient time dependence proportional to a linear combination of several exponential terms.[7] Also, at the low-temperature end of the Raman relaxation region, a T_1 mechanism proportional to T^{-5} may be dominant.[8] These cases, however, are somewhat specialized examples of rare-earth-ion relaxation.

To evaluate T_1 from the expressions in Eqs. (1)–(6) the matrix elements of $V_n{}^m$ are required. For the rare earths, one need only consider n even and ≤ 6. Which components of $V_n{}^m$ enter into the calculation of the relaxation time in a given crystalline environment can be determined from a normal-mode analysis[2] of the vibrations of the paramagnetic ion and the nearest-neighbor surrounding charges, these being assumed to generate the principal orbit-lattice coupling. The vibrational modes transform as some combination of the irreducible representations of the crystal symmetry group. For CaF_2, which has cubic symmetry, the vibrational motion of the rare-earth ion and the eight nearest-neighbor F^- ions transform according to the following irreducible representations of the O_h group:

$$\Gamma_{\text{vib}}(O_h)=A_{1g}+A_{2u}+E_g+E_u+2T_{1u}+2T_{2g}+T_{2u}, \quad (7)$$

where for transitions within a given electronic configuration only the even vibrations need be considered and the translational and rotational terms have been subtracted out. Similarly, for the tetragonal and trigonal site symmetries described previously,[5]

$$\Gamma_{\text{vib}}(C_{4v})=5A_1+A_2+2B_1+4B_2+6E, \quad (8)$$

and

$$\Gamma_{\text{vib}}(C_{3v})=6A_1+A_2+7E. \quad (9)$$

Comparison of the irreducible representations in (7), (8), and (9) and those according to which the $V_n{}^m$'s transform, shows that in all cases the vibrational motion is factored into a number of representations such that all $V_n{}^m$'s are allowed. Thus there is no reduction and simplification in the number of terms which must be considered in applying the above theoretical expressions to the evaluation of T_1 for ions in the different symmetry sites in CaF_2.

Attempts to make explicit calculations of spin-lattice relaxation times are plagued by the necessity of making numerous assumptions and approximations. Given expressions for T_1 as in Eqs. (1)–(6), which are derived using a simplified treatment of the lattice vibrations, estimates must be made of the dynamic crystal-field components. Two approximations which have been used[2,3] in making such estimates are that (1) the orbit-lattice interaction parameters may be approximated by static crystal-field parameters, i.e., $|(x\partial A_n{}^m/\partial x)| \approx |A_n{}^m(x_0)|$, where x is a ligand coordinate displacement, and (2) $|A_n{}^m| \approx |A_n{}^0|$. Although the latter rule was based upon empirical data, it is not universally satisfied. Other approaches[9] include estimates of the strength of the orbit-lattice parameters obtained from uniaxial stress and ultrasonic spin-phonon absorption experiments. Convincing calculations of the parameters would require knowledge of the nature of the ligand fields, shielding effects, and vibrational motion. In the following we shall consider those combinations of matrix elements of the orbit-lattice interaction which appear in the expressions for the direct, Orbach, and Raman T_1's as parameters to be determined experimentally. These are compared later with rough order-of-magnitude estimates using the above approximations and the crystal-field parameters and energy level splittings found in I.

For a resonance frequency of 9.6 kMc/sec and taking $\rho=3.18$ g/cm^3 and a mean phonon velocity, $v=4\times10^5$ cm/sec for CaF_2, T_1 for the direct process in Eq. (1) becomes

$$T_{1D}=(1.5/TM_D{}^2)(\text{sec}), \quad (10)$$

where for non-Kramers ions,

$$M_D{}^2\equiv|\langle a|\sum_{n,m} V_n{}^m|b\rangle|^2(\text{cm}^{-2}), \quad (11)$$

and for Kramers ions,

$$M_D{}^2\equiv(2\beta\Lambda/\Delta_c)^2\{|\langle a|\mathbf{H}\cdot\mathbf{J}|c\rangle\langle c|\sum_{n,m} V_n{}^m|b\rangle + \langle a|\sum_{n,m} V_n{}^m|c\rangle\langle c|\mathbf{H}\cdot\mathbf{J}|b\rangle|\}^2(\text{cm}^{-2}). \quad (12)$$

For the Orbach process, from Eq. (3),

$$T_{1O}\approx\frac{\exp(\Delta_c/kT)}{4\Delta_c{}^3(\text{cm}^{-3})M_O{}^2}(\text{sec}), \quad (13)$$

where

$$M_O{}^2\equiv\frac{|\sum_{\substack{n,m\\n',m'}}\langle a|V_n{}^m|c\rangle\langle c|V_{n'}{}^{m'}|b\rangle|^2}{|\sum_{n,m}\langle a|V_n{}^m|c\rangle|^2+|\sum_{n'm'}\langle c|V_{n'}{}^{m'}|b\rangle|^2}(\text{cm}^{-2}). \quad (14)$$

A summation is to be made over all effective excited states $|c\rangle$ in (12) and (14). For Kramers salts, the T^{-9} Raman relaxation mechanism in Eq. (5) is usually dominant and reduces to

$$T_{1R}\approx(10^7\Delta^4/T^9M_R{}^4)(\text{sec}), \quad (15)$$

where

$$M_R{}^2\equiv|\sum_{\substack{n,m\\n',m'}}\langle a|V_n{}^m|c\rangle\langle c|V_{n'}{}^{m'}|b\rangle|(\text{cm}^{-2}). \quad (16)$$

[7] R. W. Bierig and M. J. Weber, Phys. Rev. **132**, 164 (1963).
[8] R. Orbach and M. Blume, Phys. Rev. Letters **8**, 478 (1962).
[9] M. Blume and R. Orbach, Phys. Rev. **127**, 1587 (1962).

Scott and Jeffries[3] found from the actual computation of sums of the type $\sum_{n,m}|\langle a|V_n{}^m|c\rangle|^2$ (assuming the individual terms to be incoherent), that for several rare earths these sums were of the same order of magnitude. Thus one might expect that $M_D{}^2$ (allowing for Zeeman admixing), $M_O{}^2$, and $M_R{}^2$ would not differ greatly. Exceptions are always possible, however, and would depend upon the actual state wave functions. Note, also, that if the magnitudes of $|\sum\langle a|V_n{}^m|c\rangle|^2$ and $|\sum\langle c|V_n{}^m|b\rangle|^2$ in Eq. (14) are very different, $M_O{}^2$ will be determined by the smaller of the two.

EXPERIMENTAL

A schematic representation of the pulse saturation X-band spectrometer used in measuring spin-lattice relaxation is shown in Fig. 1. The principles of operation are straightforward. A VA 153 reflex klystron is used as a main rf power source. The klystron environment is a temperature-stabilized oil bath, an important improvement for obtaining good low-noise klystron operation. The VA 153 is frequency stabilized to the sample cavity resonance. Relatively high-power rf pulses are generated by two states of X-band amplification obtained using VA 824B klystron amplifiers driven by the VA 153. The rf pulse width can be varied from 2–500 μsec and peak output power is ≈ 20 W. Klystron amplifiers have the advantage that their output pulse is monochromatic to the extent that the driving element is frequency stabilized, hence there are no high-peak power FM signals reflected from the sample cavity to interfere with detection of the low-level transient relaxation signals. A portion of the VA 153 output is used as a low-level cw monitor of the sample cavity reflection coefficient. The cw power level incident on the sample cavity is normally kept between 0.1 and 10 μW.

The transient signals generated by relaxation of the spin system, following a high-power saturating pulse, are detected in a standard mixer; subsequent amplification is performed at 30 mc, the difference frequency at which the local oscillator is stabilized. The transient relaxation signals are displayed on a Tektronix oscilloscope and photographed. The VA 153 stabilization loop has a variable bandwidth (1–100 kc/sec) to permit rapid correction of the output frequency so that the sample cavity may be transiently tracked. If this is not done and care is not exercised so that the sampling frequency is at the center of cavity resonance, a mixture of time-dependent absorption and dispersion may be detected. The decay times of the real and imaginary components of the reflection coefficient are not necessarily the same, hence considerable confusion in the data may occur if this admixture is not taken into account. An alternative to rapid stabilization is to measure the decay time of the observed transient signal far out in the tail where the dispersion is small.

Diminution of pulse power incident on the mixer is accomplished by synchronously switching a double-diode switch to reflect pulse power back into an absorbing isolator. The time resolution of the spectrometer, which is a few microseconds, is determined by the "turn-off" time of the klystron pulse amplifiers and by the recovery time of the preamplifier "front end" from saturation.

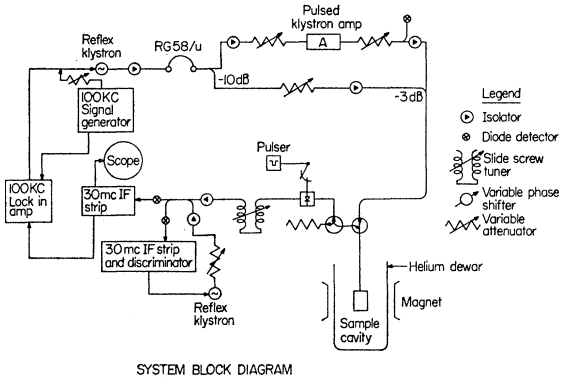

FIG. 1. Schematic diagram of pulse saturation X-band spectrometer.

The sample cavity resonates in the TE011 circular electric mode and has a loaded $Q \approx 8000$–10 000. The sample under study is mounted axially in the resonant chamber on a sapphire tube. At low temperatures the sapphire provides excellent thermal coupling to the cavity which, in turn, is in thermal contact with the helium bath via helium exchange gas. The cavity mass acts as the thermal reservoir to which the spin system relaxes. The cavity temperature is carefully monitored by a set of 3 thermometers; two 47-Ω carbon resistors and a platinum resistance thermometer. The carbon resistors were individually calibrated between 1.5 and 20°K; the platinum resistance thermometer was calibrated from 4.2–300°K. These three thermometers were used together with a gold-cobalt differential thermocouple connected between one of the carbon resistors and the sample mount to verify that the sample temperature did indeed track the cavity temperature in the range 2–50°K. The maximum temperature differential was found to be less than 0.1°K in this temperature range. This was important, since all relaxation measurements at temperatures above 4.2°K were made by simply allowing the cavity structure to warm toward 77°K. The total time available for measurements between 4.2 and 50°K is typically 3.5 h.

Most of the CaF_2 crystals used in these experiments were grown in this laboratory by the Czochralski method[10a] or by a modified Stockbarger[10b] technique. The melts were contained in molybdenum crucibles and the growth ambient consisted of dry argon gas [dew point < -100°F]. Other samples were purchased from Optovac, Inc. The crystals were annealed by sealing them in evacuated quartz ampoules [10^{-6} mm Hg at

[10] (a) K. Nassau, J. Appl. Phys. **32**, 1820 (1961). (b) D. C. Stockbarger, J. Opt. Soc. Am. **39**, 731 (1949).

20°C], heating them to 1200°C for 12 h, followed by slow cooling at ~20°C/h. In general, the samples had rare-earth dopings of the order of 0.1 wt.%; undesirable impurities were present $\lesssim$0.001 wt.% as determined from spectrographic analysis. Each sample was x-ray oriented to within ±2° of the desired orientation. The typical sample size was approximately 0.1×0.1×0.3 cm, which gave a cavity filling factor of about 0.001.

Except where noted, the observed transient relaxation signals exhibited a single exponential time dependence. T_1 was obtained from a semilog plot of signal amplitude versus time and was defined as the time at which the signal had recovered to $(1-e^{-1})$ of its equilibrium value. The experimental uncertainty in the individual T_1 determinations is typically ~10%. The electron paramagnetic resonance (EPR) spectrum was examined as a function of cw power level to insure that the sampling signal intensity was always at least 20 dB below the power level at which steady-state saturation could be observed. For a few of the samples (Ce^{3+} and Gd^{3+}) the incident power had to be reduced to a few tenths of a microwatt. The saturating pulse width τ_p was always adjusted such that $\tau_p \lesssim T_1$.

RESULTS

Cerium

Spin-lattice relaxation of Ce^{3+} in tetragonal sites in CaF_2 was investigated in the temperature range 2–15°K for five samples having different Ce concentrations ranging from 0.08 to 1.6 wt.% cerium. In all samples the tetragonal site resonances were the most intense. Additional lines were usually present in the resonance spectrum, particularly at the higher Ce concentrations (see Fig. 2 of I); however, they were generally too weak for relaxation measurements. T_1 measurements were made with the magnetic field H applied in a (100) crystallographic plane.

Figure 2 shows the over-all temperature dependence of T_1 for several different Ce^{3+} concentrations. The transient recovery from saturation of the signal from the 1.6% sample displayed a single exponential time dependence with a characteristic time which was approximately temperature-independent at low temperatures. The recovery of the other samples, however, could not be fitted by a single exponential term at low temperatures but rather by a sum of two or three exponential terms. An initial rapid recovery was usually observed which was more or less temperature-independent but concentration-dependent. This component had a characteristic time varying from ≈100 μsec for the 0.34% sample to ≈300 μsec for the 0.08 and 0.18% samples. When saturation pulses of several hundred microseconds duration were applied, this component was diminished. Thus it appears to be associated with the establishment of internal equilibrium within the spin system[11] and not

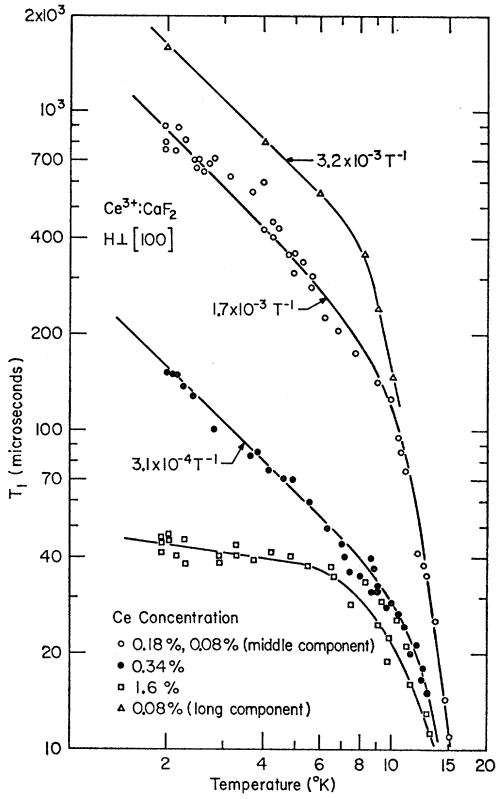

FIG. 2. Temperature dependence of relaxation time T_1 of Ce^{3+} in tetragonal sites in CaF_2 for several different Ce concentrations.

spin-lattice relaxation. Following it was a temperature-dependent recovery composed of one or two exponential terms. The dominant temperature-dependent component of the recovery is concentration-dependent and is plotted as T_1 in Fig. 2. A final rather weak temperature-dependent component of the recovery is also plotted in Fig. 2 for the 0.08% sample. Except for the most concentrated 1.6% sample, the relaxation in the low-temperature region is characterized by a T^{-1} temperature dependence and a concentration-dependent magnitude.

At higher temperatures, $T>10$°K, the data for the different samples tend to converge to a value independent of the cerium concentration. The asymptotic T_1 temperature dependence can be fitted to a T^{-9} law for Raman relaxation of a Kramers ion using $T_{1R}\approx 4\times 10^5\ T^{-9}$ sec. The data can also be fitted to an exponential law with $\Delta\sim 150$ cm^{-1}; however, the fit is poorer.

For several of the rare-earth ions studied it is difficult to establish an unambiguous temperature dependence at high temperatures since the magnitude of T_1, after subtracting out the T^{-1} dependence at low temperatures is not known accurately over a sufficiently broad range of temperature.

If the asymptotic T_1 temperature dependence is fitted to be a T^{-9} law for Raman relaxation, we find from Eq. (15) that $M_R^2\approx 5\Delta^2$. The first excited state for Ce^{3+}

[11] K. D. Bowers and W. B. Mimms, Phys. Rev. **115**, 285 (1959).

in tetragonal sites should be of form $|\pm\frac{1}{2}\rangle$. Sums of the type $\sum|\langle a|V_n^m|c\rangle|^2$ connecting this state to the ground state have values $\approx 1.5\times10^4$ cm^{-2} for $A_2^m\langle r^2\rangle\sim200$ cm^{-1} and $A_4^m\langle r^4\rangle\sim400$ cm^{-1}. (More correct wave functions, including admixtures of states from $^2F_{7/2}$, would introduce terms involving V_6^m; however, they are not expected to change the order of magnitude of the above result.) An M_R^2 of this magnitude, however, implies a small Δ which is inconsistent with the dominance of Raman relaxation. If we consider Orbach relaxation via an excited state at ~150 cm^{-1}, we find from the data and Eq. (13), $M_O^2\sim10^4$ cm^{-2}. Although the fit to an exponential temperature dependence is poorer, the magnitude agreement is better. A comparable Raman relaxation rate for $\Delta\sim150$ cm^{-1} requires orbit-lattice matrix elements $M_R^2\sim10^5$ cm^{-1}. Although there is a large uncertainty in our estimates of the V_n^m's, the above values of M_O^2 and M_R^2 are not unreasonable. Also an excited-state separation of a few hundred cm^{-1} for Ce^{3+} is possible if the tetragonal fields are as large as they appear to be for other rare earths in CaF_2.[5] Thus the above estimates are inconclusive in establishing whether the high-temperature relaxation is Raman or Orbach. The former, however, requires the larger orbit-lattice interaction.

The angular variation of T_1 with magnetic field direction in a (100) plane is shown in Fig. 3. The measurements were made using a 0.34% Ce sample at 2°K. The same ratio of T_1's for the $g_\parallel$ and $g_\perp$ resonances, i.e., for the magnetic field H applied along [100] and [010], was observed from the 0.18% sample, while for the 1.6% sample the two T_1's were equal. Since the $g_\parallel$ resonance is weaker than the $g_\perp$ resonance, the relaxation could not be measured in the former orientation for the 0.08% sample.

If the first excited tetragonal state is $|\pm\frac{1}{2}\rangle$, direct relaxation should be highly anisotropic since there is no Zeeman admixing for $\theta=0$. The over-all shape of the curve in Fig. 3, however, does not correspond exactly to that expected for an excited state of either $(\pm\frac{1}{2})$ or $(\pm\frac{5}{2}, \mp\frac{3}{2})$ and may be related to the concentration-dependent effects. The dip in T_1 near $\theta=80°$ occurs in the vicinity of the crossover of the resonances from Ce^{3+} in sites of tetragonal and trigonal symmetries. This suggests the possibility of cross-relaxation effects, although such effects are not observed when cubic and tetragonal Yb^{3+} resonances are overlapped, as we report later. Within experimental error, the relaxation at this orientation exhibited a simple exponential recovery.

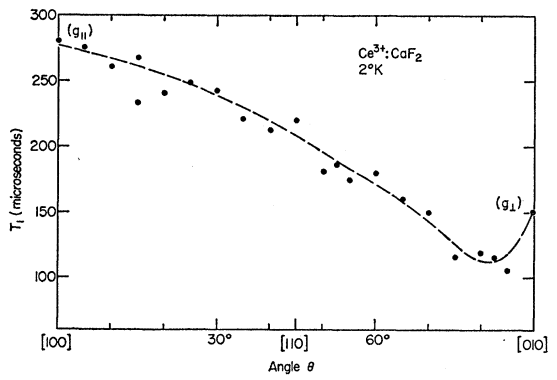

FIG. 3. Angular variation of T_1 for Ce^{3+} in tetragonal sites in CaF_2. The magnetic field is applied at an angle θ with respect to a [100] axis in a (100) plane.

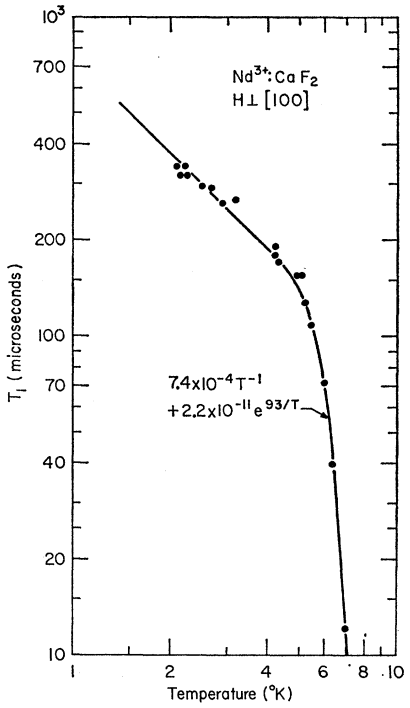

FIG. 4. Temperature dependence of relaxation time T_1 of Nd^{3+} in tetragonal sites in CaF_2. Nd concentration is 0.28%.

Neodymium

The temperature dependence of T_1 for Nd^{3+} in tetragonal sites is shown in Fig. 4, where the $g_\perp$ resonance for $H\perp[100]$ has been measured. Several weak broad ($\sim$40–100 G) lines whose origin and nature were not established were present in the resonance spectrum. At 2°K the relaxation time of the $g_\parallel$ resonance is about twice as long as that of the $g_\perp$ resonance. At low temperatures T_1 exhibits a T^{-1} dependence. At the higher temperatures, $T>4$°K, a relaxation mechanism decreasing more rapidly than T^{-9} with increasing temperature begins to dominate. It can be fitted to an exponential temperature dependence given by $T_1=2.2\times10^{-11}\exp(93/T)$ sec. This suggests relaxation via an excited state or states effectively at ≈65 cm^{-1} above the ground state. The optical fluorescence data in I indicates a first excited state at ≈90 cm^{-1}. Within experimental error the two results are probably compatible. A tetragonal crystal-field component $A_2\langle r^2\rangle$ of a few hundred cm^{-1} would greatly perturb the two cubic-field Γ_8 quartets at

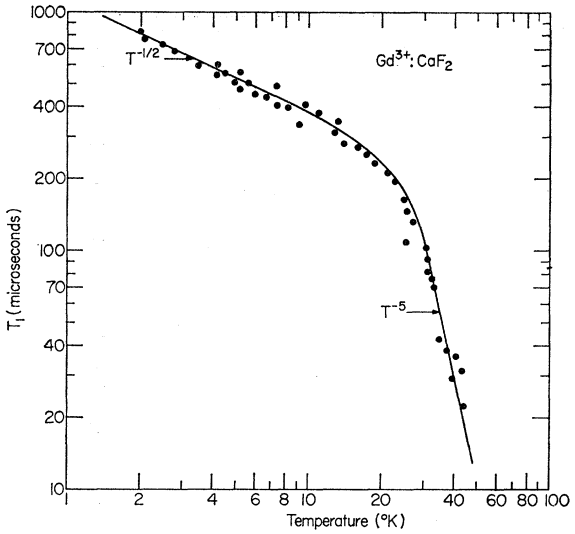

FIG. 5. Temperature dependence of relaxation time T_1 of Gd^{3+} in tetragonal sites in CaF_2. Gd concentration is 0.03%.

0 and 180 cm^{-1}, hence an energy level at 65–90 cm^{-1} is not unexpected. For Orbach relaxation via an excited state $\Delta=65$ cm^{-1}, we find from the Nd^{3+} results and Eq. (13), $M_O^2\approx 4\times 10^4$ cm^{-2}.

Gadolinium

The relaxation of Gd^{3+} ions in tetragonal sites was investigated. At liquid-helium temperatures the relaxation times of all transitions observable at X-band frequencies were essentially equal. Extensive measurements from 2 to 45°K were made of the temperature dependence of T_1 for the $\frac{1}{2}\leftrightarrow-\frac{1}{2}$ transition with $H\|[100]$ and are shown in Fig. 5. The over-all temperature dependence of the T_1 data can be fitted by $T_1=1.1\times10^{-3}$ $T^{-1/2}+4\times10^3$ T^{-5} sec. The transient recoveries were essentially single exponentials. Gadolinium ions were also present in sites of trigonal symmetry in the sample used; however, the relaxation was not examined.

Since an S state is unperturbed by a crystal field in first order, the crystal-field splittings and relaxation rates are usually very small. This is indeed observed for Gd: CaF_2, although the relaxation times below $\sim$10°K are unexpectedly short, again, as in the case of other rare-earth ions in CaF_2, less than 1 msec. This rapid T_1 and its $T^{-1/2}$ temperature dependence suggests that the low-temperature relaxation rate is not associated with the normal direct process and orbit-lattice interactions. The relaxation times at higher temperatures are longer than those for other non-S-state ions. The T^{-5} dependence may arise from two-phonon relaxation processes involving excited states within the $S_{7/2}$ multiplet[8] or relaxation of time conjugate states associated with a lattice defect site.[12] Since the measurements were made in a range where $T\lesssim 0.1\theta$ and θ_D for CaF_2 is $\approx$480°K, a $T_1\propto T^{-5}$ region is not expected at these temperatures for normal Raman relaxation processes.

Orbach and Blume[8] have shown that for a multilevel spin system at low temperatures, Raman relaxation via excited states within the multiplet will be proportional to T^{-5} and can be more important than T^{-7} and T^{-9} processes involving higher excited states. In general, when the excited-state energy is very small compared to the energy of the most important phonons for relaxation, the denominator of the second-order Raman process is $\approx(\hbar\omega_p)^2$ rather than Δ^2 as in Eq. (4). Thus one has in place of Eq. (4),

$$\frac{1}{T_{1R}}=\frac{9}{4\pi^3\rho^2v^{10}}\frac{4!}{\hbar^2}\left(\frac{kT}{\hbar}\right)^5 M_R{}^4. \tag{17}$$

$M_R{}^4$ is again given by Eq. (16), but now $|c\rangle$ is a state within the ground multiplet.

The energy levels for Gd^{3+} in a tetragonal field in CaF_2 and for a resonance frequency of 9.6 kMc/sec for the $\frac{1}{2}\leftrightarrow-\frac{1}{2}$ transition can be derived from the parameters given by Vinokurov *et al.* (see I). They form a multilevel system in which the Orbach-Blume mechanism may be operative. If the effective dynamic crystal-field interactions have the same relative importance as the static crystal-field parameters in the spin Hamiltonian, then the $b_2{}^m$ terms should dominate and Raman relaxation would proceed principally via the $|\pm\frac{3}{2}\rangle$ states. Comparison of Eq. (17) with the experimental T_1's for Gd: CaF_2 yields $M_R{}^2\approx 1.4\times10^3$ cm^{-2}. This value while smaller than for Kramers ions, is, however, several orders of magnitude larger than that predicted using the static crystal-field parameters.

Terbium

Trivalent terbium is the only non-Kramers ion studied. A plot of T_1 versus T for an $H\perp[111]$ sample orientation is shown in Fig. 6. The relaxation times of each of the four Tb^{159} hyperfine components were essentially equal. In the T^{-1} region the Tb^{3+} relaxation times are much faster than those found for the other ions. Above 4°K, T_1 exhibits a gradual departure from a T^{-1} law. By 10°K, T_1 has decreased to a value approaching the limiting resolution of the apparatus; and, accordingly, the data in this region has a larger experimental error. The data, after substraction of the T^{-1} dependence, can be fitted to an exponential law with $\Delta\sim20$ cm^{-1}; however, one cannot attach too much significance to this result due to the large experimental uncertainties involved. The location of the excited levels of $^7F_6$ in a tetragonal field have not been reported to our knowledge.

The angular variation of T_1 at 2°K and for a magnetic field applied in a (111) plane is shown in Fig. 7. Broad anisotropic resonances previously reported by Forrester

[12] J. G. Castle, D. W. Feldman, P. G. Klemens, and R. A. Weeks, Phys. Rev. **130**, 577 (1963).

and Hempstead[13] in Tb:CaF_2 were also observed in the sample used. The presence of Tb^{3+} in sites of trigonal symmetry, which are not observable at X-band frequencies, was not established.

Terbium, being a non-Kramers ion, is expected to relax faster at low temperatures than Kramers ions, which is indeed observed. The M_D^2 determined from Eq. (10) is $\approx 3\times 10^4$ cm^{-2}. The resonant doublet, however, is composed principally of $J_z=\pm 6$ states which are not connected by the orbit-lattice interaction. Relaxation may be allowed, for example, by admixing of $J_z=\pm 2$ states. This small admixture would reduce the value of M_D^2 relative to that for other ions.

The above measurements were made in a sample containing 0.5% Tb. The relaxation from a 1.4% Tb sample was also measured between 2–4°K, where T_1 ~ 5 μsec, independent of temperature.

Dysprosium

Two different samples of dysprosium-doped CaF_2 ($\sim$0.1–0.2% Dy) each containing Dy^{3+} in sites of cubic tetragonal, and trigonal symmetries were examined. No measurable relaxation recoveries were observed from any of the resonances for temperatures 2–4°K. Based upon the limiting resolution of the apparatus, this result suggests that the relaxation times of the Dy^{3+} resonances in the samples studied are $\lesssim 3$ μsec.

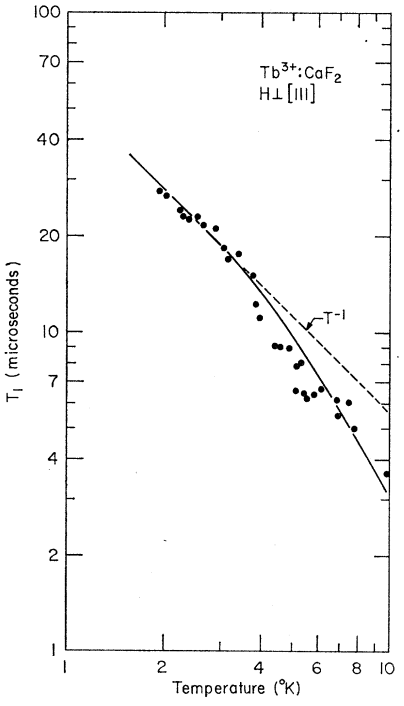

FIG. 6. Temperature dependence of relaxation time T_1 of Tb^{3+} in tetragonal sites in CaF_2. Tb concentration is 0.5%.

[13] P. A. Forrester and C. F. Hempstead, Phys. Rev. **126**, 923 (1962).

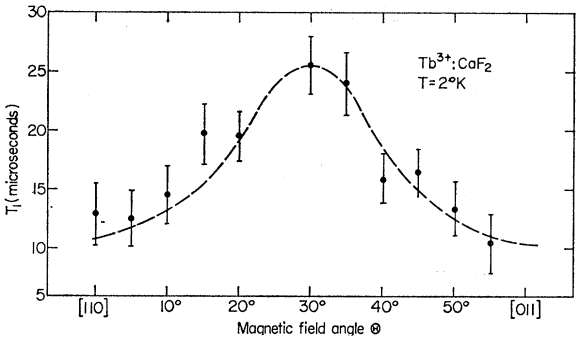

FIG. 7. Angular variation of T_1 for Tb^{3+} in tetragonal sites in CaF_2. The magnetic field is applied in a (111) plane.

The Dy^{3+} relaxation rates may be faster than those of other rare earths because of the presence of a relatively low-lying excited state. In a cubic field the relaxation of pairs of levels within the ground-state Γ_8 quartet may occur via an Orbach process involving the Γ_7 excited state at $\Delta\approx 8.5$ cm^{-1}. A T_1 of 1 μsec, which would account for the unresolved relaxation transient, is predicted at 4°K for such a process if $M_O^2\approx 10^4$ cm^{-2}. Corresponding times for Raman relaxation require $M_R^2\approx 4\times 10^5$ cm^{-2}. If this process was dominant, however, lifetime broadening of the Γ_8 resonances should be evident by $T\approx 10$°K, which is not observed. At $T=2$°K, the major relaxation mechanism may be two-step relaxation processes involving states within the Γ_8 quartet, as discussed elsewhere.[7]

The relaxation rate of the cubic field Γ_7 excited state would also be fast if the strength of the orbit-lattice interaction is as strong as required above, the temperature dependence of an Orbach process changing from a constant at low temperatures, $T\ll\Delta$, to a T^{-1} law at high temperatures. At temperatures $\lesssim 15$°K, lifetime broadening of the Γ_7 resonance linewidth is observed. From the estimated magnitude and slow temperature variation of the Γ_7 Orbach process, the broadening probably arises from the dominance of Raman relaxation at these temperatures. From Eq. (15), a T_{1R} of 10^{-9} sec, and hence line broadening, is predicted at $T=15$°K if $M_R^2\approx 4\times 10^4$ cm^{-2}.

Erbium

The temperature dependence of the relaxation of Er^{3+} in sites of tetragonal (I) and trigonal (II) symmetry are recorded in Fig. 8. The position and relative intensities of the resonances in the low-field portion of the spectrum of the 1.0% Er^{3+} sample used are shown in Fig. 5 of I for $H\|[110]$. Due to the strong overlap and relative intensities of the tetragonal (I) and cubic resonances, only a common transient decay was observed when the magnetic field was set in the region $\approx$950–1070 Oe, the amplitude varying as the magnetic field was adjusted to line center. The transient signal, which appears to be dominated by the tetragonal (I)

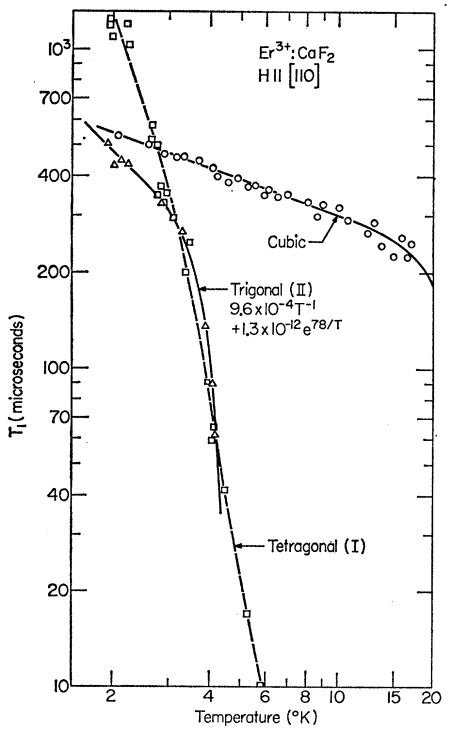

FIG. 8. Temperature dependence of relaxation time T_1 of Er^{3+} in tetragonal and trigonal sites in CaF_2. Er concentration is 1.0%. Cubic T_1 is from another sample (see text).

resonance, is characterized by a temperature-independent component (~100 μsec) and a strongly temperature-dependent component which is plotted as T_1 (tetragonal) in Fig. 8. The variation of T_1 with angle of the magnetic field in a (100) plane is at most 20%; there is no measurable variation of the initial decay component. At low temperatures, ~2°K, a third decay component is evident having a characteristic time ~2–5 msec. The amplitude of this signal, however, is so small that the experimental uncertainty in the decay time is very large.

The high-temperature portion of the tetragonal (I) T_1 versus T curve can be fitted by an exponential law given by $T_1\approx10^{-7}\exp(27/T)$ sec. At low temperatures the data deviates from the exponential curve; however, the data is not sufficient to establish a reliable temperature dependence for the competing relaxation process, which might be expected to have a $1/T$ law. An effective tetragonal excited state at ~27°K from relaxation data is not unreasonable in view of the crystal-field splittings in I and the excited state at ~35°K reported by Baker *et al.* from measurements of the temperature dependence of the intensity of the tetragonal excited-state resonance. Assuming an Orbach process is operative, the Mo^2 derived from the above result and Eq. (13) is $\approx10^3$ cm^{-2}. Line broadening of the cubic-tetragonal (I) group of resonances occurs for $T\gtrsim30$°K; by 40°K the individual lines are no longer resolvable.

The trigonal (II) relaxation was measured with the magnetic field applied in a [110] direction to separate the $g_\perp$ trigonal resonance as far as possible from the other spectral lines. The results in Fig. 8 show a T^{-1} region and a rapidly decreasing T_1 at higher temperatures which can be fitted to an exponential law. The over-all temperature dependence can be fitted by

$$T_1=9.6\times10^{-4}T^{-1}+1.3\times10^{-12}\exp(78/T)\text{ sec}.$$

Comparing this result with an Orbach process in Eq. (13) yields $Mo^2\approx10^6$ cm^{-2}. The linewidth of the trigonal (II) resonance increased rapidly for temperatures $\gtrsim25$°K and became unobservable above 30°K indicative of lifetime broadening and $T_1\lesssim10^{-9}$ sec.

T_1 measurements were made earlier[14] in another Er:CaF_2 crystal which was less heavily doped than the above sample and in which Er^{3+} ions in cubic sites were approximately twice as numerous as those in tetragonal (I) sites. T_1 data for ions in trigonal (II) sites, which were also present, agreed with the data presented above. Data taken in the vicinity of the isotropic cubic resonance is shown in Fig. 8. For this sample the tetragonal (I) resonances could not be sufficiently well isolated to yield unambiguous results. Between 2 and 15°K, T_1 for the cubic resonance exhibited very little temperature dependence and can be fitted by $T_1\propto T^{-n}$, where $n\approx\frac{1}{3}$. This rather unexpected result was reproduced under varied experimental conditions and appears to be

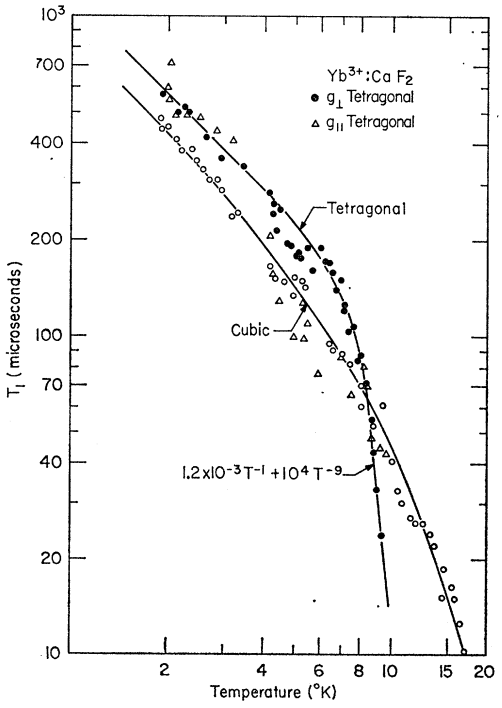

FIG. 9. Temperature dependence of relaxation time T_1 of Yb^{3+} in cubic and tetragonal sites in CaF_2. Yb concentration is 0.17%.

[14] M. J. Weber and R. W. Bierig, Bull. Am. Phys. Soc. 8, 259 (1963).

intrinsic to the sample. Since there should be cubic-field excited states within 100 cm^{-1} of the ground state, such long T_1's for $T>10°K$ are very unusual.

The relaxation of Er^{3+} in tetragonal sites in CdF_2 has been measured by Zverev *et al.*[15] at X-band frequencies, and the results are reviewed here for comparison. The Er concentration was $\sim 0.1\%$. For $T<4.2°K$, T_1 varied inversely with temperature, where $T_1 \approx 5.5\times 10^{-4}\ T^{-1}$ sec. Between 4.2 and 9°K, T_1 exhibited a rapid decrease from a T^{-1} law; lifetime broadening was observed above 16°K. Combining the last two data the authors conclude that T_1 cannot be described by a power law of the type $T_1 \propto T^{-n}$. Instead, the relaxation appears to be influenced by the presence of a nearby excited state.

Ytterbium

In Fig. 9 are shown the temperature dependences of T_1 for Yb^{3+} in cubic and tetragonal crystal fields. The resonance spectrum for this 0.17% Yb sample was very clean, consisting only of approximately equally intense cubic and tetragonal resonances. Both the $g_{\parallel}$ and $g_{\perp}$ tetragonal resonances exhibited nearly equal relaxation rates inversely proportional to T at the lowest temperatures. With increasing temperature the $g_{\perp}$ resonance T_1 decreases rapidly reaching a T^{-9} dependence by 10°K. Within experimental error, the high-temperature data may also be fitted by an exponential law with an exponent $\approx 125/T$. T_1 for the $g_{\parallel}$ resonance shows an anomalous behavior for $3.5<T<10°K$, which we do not understand at present.

The cubic resonance T_1 gradually departs from a T^{-1} law with increasing temperature. The data for $5°<T<20°K$, after subtraction of the T^{-1} dependence, can, within experimental accuracy, be fitted to either a $T^{-(3.5\pm 0.5)}$ or $\exp(38/T)$ temperature dependence. The cubic Yb^{3+} resonance is unique among the rare-earth ions studied in that it is observable up to $\approx 115°K$; the tetragonal Yb^{3+} resonances are not observable at 77°K. The temperature dependence of the cubic resonance linewidth was examined between 50–105°K. At low temperatures the peak-to-peak linewidth of the derivative of absorption is temperature-independent with a value of ≈ 25 G. The additional temperature-dependent linewidth $\Delta H(T)$ above 50°K is plotted in Fig. 10. If this width is attributed to lifetime broadening, its temperature dependence should reflect that of T_1 in this temperature range. The data in Fig. 10 shows a slow departure from a T^{-9} law. The temperature dependence for Raman relaxation of a Kramers ion, assuming a simple Debye lattice and characteristic temperature θ_D, is $T^9 \int_0^{\theta_D/T} [x^8 e^x dx/(e^x-1)^2]$, the T^9 limit applying only when $T<0.1\theta_D$. Since $\theta_D \approx 480°K$[16] for

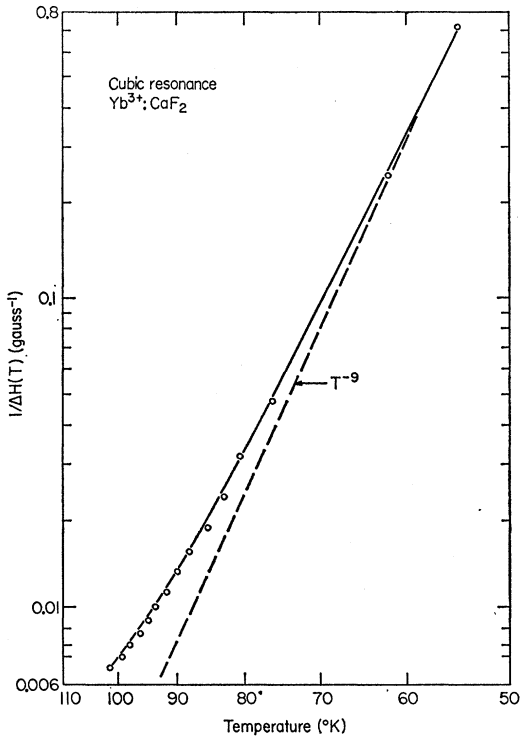

FIG. 10. Additional temperature dependence component $\Delta H(T)$ of the linewidth of Yb^{3+} in cubic sites in CaF_2.

CaF_2, the deviation from T^{-9} is expected; however, it should be more pronounced. The above integral expression with $\theta_D \sim 680°K$ provides a better fit to the data. There are several possible sources of this discrepancy; the validity of considering $\Delta H(T)$ as a simple additive contribution, the inadequacy of a simple Debye vibrational frequency spectrum for CaF_2 and the above integral expression,[17] and the possible enhanced Raman relaxation rate due to the mass excess of the rare-earth impurity.[18]

From estimates in I (see Fig. 5), the first excited state for Yb^{3+} in a cubic field in CaF_2 may be ≈ 600–$700\ cm^{-1}$ above the ground state. Thus T_{1R}, which is proportional to Δ^4, would be much longer than for other rare earths. This would account for the cubic-field resonance being observable at such comparatively high temperatures. Since a Δ of this size is probably greater than the highest energy branch in the phonon spectrum of CaF_2, a simple Orbach process would not be allowed. Comparing the observed broadening with Raman relaxation, a value of $M_R^2 \approx 10^5\ cm^{-2}$ is obtained, which is necessarily uncertain due to the lack of good agreement in fitting the temperature dependence. Extrapolating this relaxation mechanism for $T=10-20°K$ yields T_1 values several orders of magnitude longer than observed. If the higher

[15] G. M. Zverev, L. S. Kornienko, A. N. Prokhorov, and A. I. Smirnov, Fiz. Tverd. Tela **4**, 392 (1962) [English transl.: Soviet Phys.—Solid State **4**, 284 (1962)].

[16] D. R. Huffman and M. H. Norwood, Phys. Rev. **117**, 709 (1960).

[17] M. J. Weber, Phys. Rev. **130**, 1 (1963).

[18] J. G. Castle, Jr., D. W. Feldman, and P. G. Klemens, *Advances in Quantum Electronics* (Columbia University Press, New York, 1961), p. 414.

temperature T_1's for the tetragonal resonances are fitted to a T^{-9} law, Eq. (15) gives $M_R^2 \approx 30\Delta^2$. A tetragonal field is not expected to split the Γ_8 excited state of $^2F_{7/2}$ by more than a few hundred cm^{-1}. This would again suggest a relatively large first excited-state separation for the tetragonal ion relaxation and would require very large values of M_R^2, $\lesssim 10^6$ cm^{-2}, to account for the observed T_1's. Orbach relaxation, on the other hand, via an excited state at ≈ 100 cm^{-1}, as suggested from the T_1 temperature dependence, would require $M_O^2 \approx 10^5$ cm^{-2}.

Good agreement was generally obtained for T_1 measurements from several different Yb:CaF_2 samples. No effects were observed which suggested the presence of any cross-relaxation between the Yb resonances. For $H \| [100]$, all transient signals displayed a single exponential time dependence. By varying the angle of H with respect to [100], it was possible to gradually superimpose the cubic and tetragonal resonances, at which point a short decay attributable to the cubic line and a longer decay attributable to the tetragonal line were observed. Although the uncertainty in measuring the decay times in this case is greater than when either of the transients is observed separately, the measurements are of sufficient accuracy to permit identification.

Measurements of the relaxation of Yb^{3+} in cubic sites in CdF_2 at X-band frequencies have been reported.[19] At liquid helium temperatures the relaxation of a 0.1% Yb sample is described by $T_1 = (6.7 \pm 0.7) \times 10^{-4}\, T^{-1}$ sec. No resonances were observed at liquid hydrogen temperatures. More recent investigations[20] at 3.2 and 9.1 kMc/sec in samples containing 0.01, 0.05, and 0.1% Yb demonstrate that resonances are observable at 57°K. The low-temperature relaxation times are concentration-dependent as we have noted for Ce^{3+} and show an unexpected and unexplained dependence upon resonance frequency, $T_1 \propto \delta$. From g shift, intensity and optical measurements, an excited state at $\simeq$50–70 cm^{-1} and an over-all $^2F_{7/2}$ splitting of ≈ 116 cm^{-1} is inferred. These values are much smaller than those estimated for Yb:CaF_2.

DISCUSSION

The magnitude and temperature dependence of T_1's for Kramers ions at higher temperatures, where T_1 deviates from a T^{-1} law, have been compared with theoretical expressions for two-phonon relaxation processes in Eqs. (13)–(16). A single excited state was considered with an energy Δ obtained either from the exponential temperature dependence for Orbach relaxation or from estimates in I. The experimental results indicate that for Orbach and Raman relaxation, the effective sums of orbit-lattice matrix elements M_O^2 and M_R^2 are typically in the order of 10^4–10^5 cm^{-2}. These values are comparible with those obtained using the static crystal-field parameters in I and the approximations discussed earlier relating them to the strength of the orbit-lattice coupling. The accuracy of the determination of M^2 is dependent upon estimates made in arriving at Eqs. (10), (13), and (15). For example, since the average phonon velocity v enters to the fifth and tenth powers, respectively, in the Orbach and Raman T_1's, a small error in the choice of an effective v can greatly affect the magnitude of the predicted T_1. Because of this and the uncertainty in Δ, only the magnitude of M^2 is significant.

TABLE I. Comparison of low-temperature relaxation times and impurity concentration for several rare earths in tetragonal sites in CaF_2. The rare-earth concentration is the total concentration, not the number in the particular axial site.

Ion	Concentration (%)	T_1T (sec °K)
Ce^{3+}	0.08	3.2×10^{-3}
Yb^{3+}	0.17	1.2×10^{-3}
Ce^{3+}	0.18	1.7×10^{-3}
Nd^{3+}	0.28	7.4×10^{-4}
Ce^{3+}	0.34	3.1×10^{-4}
Tb^{3+}	0.5	5.5×10^{-5}
Ce^{3+}	1.6	4×10^{-5} (2–4°K)

The above value of M^2 should be useful in estimating the magnitude and dominant relaxation process for other rare earths in CaF_2 when the excited-state energies are known. It should be noted, however, that some apparent discrepancies exist. M_O^2 for the tetragonal (I) and trigonal (II) Er resonances are very different and are beyond the extremes of the above range of M^2 values. The large M_O^2 for the trigonal resonance may arise from the strong crystalline fields associated with the O^{2-} substituted at a nearest-neighbor F^- site; however, Er was the only ion in a trigonal site whose relaxation was studied, and hence this conjecture could not be verified. The relaxation of Yb in cubic sites at temperatures 10–20°K is inconsistent with the magnitude and temperature dependence of normal two-phonon processes, if our picture of the energy levels is correct. Enhanced relaxation rates having different temperature dependences arising from the presence of lattice defects and paramagnetic empurities have been discussed[12]; however, for a Kramers salt a T^{-5} dependence is expected which is beyond the estimated error of the temperature dependence for Yb^{3+}. The relaxation may be associated with the same mechanism responsible for the low-temperature relaxation discussed below.

When Eqs. (10)–(16) are compared with measured T_1's for Kramers ions, it is immediately apparent that the present theory is insufficient to account for the fast relaxation times observed in the low-temperature region, $T \lesssim 4$°K, where T_1 is usually proportional to T^{-1}. As an estimate, consider a Zeeman admixing coefficient $(2\beta\Lambda/\Delta)\langle a|\mathbf{H}\cdot\mathbf{J}|c\rangle \approx 10^{-2}$ and sums $\sum|\langle a|V_n{}^m|c\rangle|^2 \approx 10^5$ cm^{-2}. Substitution into Eqs. (10) and (12) yields

[19] V. K. Konyukhov, P. P. Pashimin, and A. M. Prokhorov, Fiz. Tverd. Tela 4, 246 (1962) [English transl.: Soviet Phys.—Solid State 4, 175 (1962)].

[20] P. P. Pashinin and A. M. Prokhorov, *Paramagnetic Resonance* (Academic Press Inc., New York, 1963), p. 197.

$T_{1D} \approx 0.1$ sec for Kramers ions at 2°K compared to observed values of ≈ 1 msec. If one assumes that the effective summations of dynamic crystal field matrix elements in direct, Orbach, and Raman relaxation have approximately equal values, i.e., M_D^2 (non-Kramers) $\sim M_O^2 \sim M_R^2$, then the predicted relative magnitudes of the one- and two-phonon relaxation processes are incompatible with experiment. In the case of Ce^{3+}, the value of T_1 at low temperatures is concentration-dependent. A tabulation of T_1T for other rare earths in CaF_2 is given in Table I and shows a correlation with rare-earth concentration. (Concentration-dependent T_1's have been observed in other crystals containing rare-earth and iron transition group elements.[21]) Finally, equally fast low-temperature T_1's have been reported for trivalent rare earths in CdF_2[15,19] and for divalent rare earths in CaF_2.[22,23] Therefore, although the relaxation times at low temperatures generally exhibit a T^{-1} dependence characteristic of one-phonon processes, their magnitude and concentration dependence indicate that they are not derived from normal direct relaxation arising from orbit-lattice interactions.

An adequate explanation of the fast low-temperature relaxation rates of trivalent rare-earth ions in CaF_2 must account for the T^{-1} dependent of T_1, the concentration-dependent effects, the variation of T_1 with angle of the applied magnetic field, and the absence of any apparent phonon bottleneck. Also, the fast relaxation has been observed for Kramers ions in lattice sites having cubic, tetragonal, and trigonal crystal-field symmetries.

The possibility exists that some divalent rare-earth ions may be introduced into CaF_2 along with the trivalent ions. If they are non-Kramers ions, they should relax quickly and could possibly influence the relaxation of trivalent Kramers ions via cross-relaxation. This explanation is insufficient for several ions studied, however, since the accompanying non-Kramers ions have nonmagnetic ground states, an example is Yb^{2+} which is isoelectric with diamagnetic Lu^{3+} ($^1S_0$). Divalent ion resonances were not readily apparent in the resonance spectrum. (Cross-relaxation could occur to excited state doublets, however, depending upon Δ, they would be depopulated at low temperatures which would reduce their effectiveness.) Finally, the orbit-lattice coupling for divalent ions would probably be less than for equivalent trivalent ions due to the smaller effective nuclear charge.

Enhanced relaxation rates may be caused by local vibration amplitude variations associated with the introduction of the paramagnetic impurity. In our case, this lattice defect has both a mass and charge difference and, for axial sites, has related substitutional or interstitial impurity defects. The relaxation would exhibit a T^{-1} temperature dependence and be a function of impurity concentration in certain ranges. Although some studies have been made of relaxation associated with defect sites,[12,24,25] detailed calculations applied to specific examples are needed to establish the importance of this mechanism at low temperatures where one-phonon processes are dominant.

Multiexponential transient recoveries were frequently observed at low temperatures in the T^{-1} region. We shall consider two cases where such behavior may be expected, cross-relaxation within an inhomogeneous spin system and cross-relaxation to another faster relaxing spin system. If a short, intense rf pulse applied to an inhomogeneously broadened spin system excites only a portion of it, then a decay time associated with the attainment of internal equilibrium within the total spin system may exist in addition to the time required to attain equilibrium with the lattice. The linewidths of rare earths in CaF_2 are usually larger than calculated dipolar widths and are believed to be inhomogeneously broadened. Several ions show transient recoveries from rf saturation having an initial fast temperature-independent but concentration-dependent exponential component. As the rf excitation pulse is lengthened, the initial recovery component became less prominent relative to the longer temperature-dependent component ascribed to spin-lattice relaxation. For Ce^{3+} at low temperatures, the initial component has characteristic times of ≈ 300, 130, and 40 μsec, respectively, for Ce concentrations of 0.18, 0.3, and 1.6%. This dependence is qualitatively as expected from the cross-relaxation theory of Bloembergen *et al.*[26]

If some paramagnetic species having a faster spin-lattice relaxation time is present, rare-earth ions in CaF_2 may lose their energy more rapidly via cross-relaxation to the other system than by relaxing directly to the lattice. Depending upon the nature of the fast relaxing system and the relative spin-lattice and cross-relaxation rates, an observed T_1 having a variety of concentration and temperature dependences can be obtained.[27–30] Rannestad and Wagner[30] have discussed some simple rate equations and time-dependent solutions pertinent to the expected behavior of such coupled spin systems. The reader is referred to their article,

[21] See, for example, papers in *Quantum Electronics* (Columbia University Press, New York, 1960); *Advances in Quantum Electronics* (Columbia University Press, New York, 1961); S. A. Peskovatskii and A. N. Chernets, Fiz. Tverd. Tela **4**, 665 (1962) [English transl.: Soviet Phys.—Solid State **4**, 484 (1962)]; A. A. Manenkov and A. M. Prokhorov, Zh. Eksperim. i Teor. Fiz. **38**, 729 (1960) [English transl.: Soviet Phys.—JETP **11**, 527 (1960)] and Ref. 29.

[22] E. S. Sabisky and H. R. Lewis, Proc. IEEE **51**, 53 (1963); H. R. Lewis and E. S. Sabisky, Phys. Rev. **130**, 1370 (1963).

[23] C. Y. Huang (private communication).

[24] B. I. Kochelaev, Dokl. Akad. Nauk SSSR **131**, 1053 (1960) [English transl.: Soviet Phys.—Doklady **5**, 349 (1961)].

[25] P. G. Klemens, Phys. Rev. **125**, 1795 (1962).

[26] N. Bloembergen, S. Shapiro, P. S. Pershan, and J. O. Artman, Phys. Rev. **114**, 445 (1959).

[27] J. H. Van Vleck, *Advances in Quantum Electronics* (Columbia University Press, New York, 1961), p. 388.

[28] J. C. Gill and R. J. Elliott, *Advances in Quantum Electronics* (Columbia University Press, New York, 1961), p. 399.

[29] N. Bloembergen and P. S. Pershan, *Advances in Quantum Electronics* (Columbia University Press, New York, 1961), p. 373.

[30] A. Rannestad and P. E. Wagner, Phys. Rev. **131**, 1953 (1963).

pp. 1958–1960, for an example of the type and range of arguments that can be presented to explain T_1 results. Their general extension to rare-earth-ion relaxation in CaF_2 is straightforward and will not be repeated here.

Although qualitative agreement might be obtained for our CaF_2 results using the above approach and appropriate models, it would be less than convincing without some knowledge regarding the origin and nature of the fast-relaxing species. The presence of other paramagnetic impurities, particularly fast-relaxing iron transition-group elements, could be important for relaxation. These impurities, however are definitely present in concentrations of less than one part in 10^4 by weight as determined by spectrochemical analysis. No distinct resonances characteristic of such ions were generally observed, although they may have been broad and hence escaped detection. Pairs, possibly exchange coupled, or clusters of rare-earth ions may be present and may account for some of the additional spectral lines observed in CaF_2 at higher rare-earth concentrations. Relaxation transitions between relatively near non-time-conjugate states associated with such clusters could be very rapid. Finally, fast relaxing centers may also be associated with the zero-field resonances noted[5,31] in Ce:CaF_2.

If the temperature-dependent relaxation times at low temperatures are characteristic of some fast-relaxing species, then the cross-relaxation time must be very fast and not the over-all relaxation bottleneck. The results for Ce^{3+}, however, show that for 1.6% Ce, an approximately temperature-independent time of ≈ 45 μsec is observed at 2–4°K suggestive of a cross-relaxation bottleneck. When the spin-lattice and cross-relaxation rates have comparable magnitudes, the relaxation of the coupled spin systems is expected to exhibit a multiexponential decay in which the relative importance of each term and its characteristic decay rate will be a function of the lattice temperature.

Until more is known about the numerous, concentration dependent lines in the EPR and optical spectra of rare-earth ions in CaF_2 and the importance of other paramagnetic impurities, the above explanation of the fast low-temperature relaxation times via cross-relaxation to other spin systems is only speculative, albeit a reasonable possibility at present.

[31] D. E. Kaplan, Bull. Am. Phys. Soc. 8, 468 (1963).

CONCLUSIONS

We have surveyed the temperature dependence of spin-lattice relaxation of several trivalent rare earths in CaF_2. The relaxation times of Kramers ions at low temperatures, which usually vary as T^{-1} and exhibit a concentration dependence, are about two orders of magnitude faster than predicted for orbit-lattice coupling. The nature of the operative relaxation mechanism which explains these results remains to be established. More intensive, detailed study of selected examples would be helpful. The magnitude and temperature dependence of two-phonon relaxation processes are generally in reasonable order-of-magnitude agreement with predictions of relaxation times using estimated crystal-field interactions. As expected, ions in lattice sites having different crystal-field symmetry and strength have different relaxation properties. The comparison between theory and experiment must of necessity be only approximate since current spin-lattice relaxation theory involves a simplified treatment of the lattice vibrational properties, but more important for rare earths in CaF_2, detailed knowledge of the energy levels, ion wave functions, and strength of the dynamic crystal field are lacking. The interpretation of the present results will benefit greatly as spectroscopic data on the crystal-field energy levels becomes available, at which time many uncertainties in the present comparison of theory and experiment will be removed.

ACKNOWLEDGMENTS

Arnold Fine's assistance in all phases of gathering the experimental data was very valuable, and the able efforts of Frederick G. Garabedian in the preparation and growth of the single crystals are greatly appreciated. Also we acknowledge valuable discussions with C. D. Jeffries, D. E. Kaplan, Z. Kiss, W. Low, P. Nutter, and L. Rimai.